Flow-driven chemistry

Guo-Hua HU

University of Lorraine - CNRS, Laboratory of Reactions and Process Engineering (UMR CNRS 7274), EEIGM-LRGP, 1 Rue Grandville, BP 20451, 54001 Nancy, France.

E-mail: guo-hua.hu@univ-lorraine.fr

ABSTRACT

Chemical reactions are often carried out under mixing, especially at an industrial scale. Mixing aims to homogenize the concentrations and temperatures of reactants over a whole reactor, and therefore often requires a 3D flow and sometimes a 2D flow. This mixing-driven-chemistry ignores or does not have to consider the effects of flow/mixing on reaction kinetics and/or selectivity because flow/mixing is likely not strong enough to significantly drive molecules from their equilibrium conformations to non-equilibrium ones. This article proposes flow-driven-chemistry which aims at manipulating the dynamics and structural order of molecules (conformation, alignment, diffusion and collision) through a strong 1D flow in order to tune the reaction kinetics and/selectivity. It describes the scientific and technical bases of flow-driven chemistry as well as its scientific and technical challenges. It provides the state of the art of the understanding related to flow-driven chemistry and perspectives for future developments.

Keywords: flow-driven chemistry, static chemistry, mixing-driven chemistry, flow chemistry, chemical reaction kinetics, chemical reaction selectivity, unidirectional flow, molecular stretching, molecular alignment.

1. INTRODUCTION

According to the collision theory, a chemical reaction between molecules is a process in which molecules must collide with each other in some way to break some of their bonds so that new bonds and therefore new molecules can be formed. Not all collisions between molecules lead to a chemical reaction. A chemical reaction kinetic constant (k) is a product of three intrinsic parameters: collision frequency between molecules (f_c), fraction of collisions with proper direction for reaction (f_d), and fraction of collisions with sufficient energy for reaction (f_e). This is described by Equation 1:

$$k = f_c f_d f_e = f_c f_d e^{-\Delta E/RT} \quad (1)$$

where ΔE is the energetic barrier called activation energy that molecular collisions should overcome in order to break bonds, R is the gas constant and T is the absolute temperature.

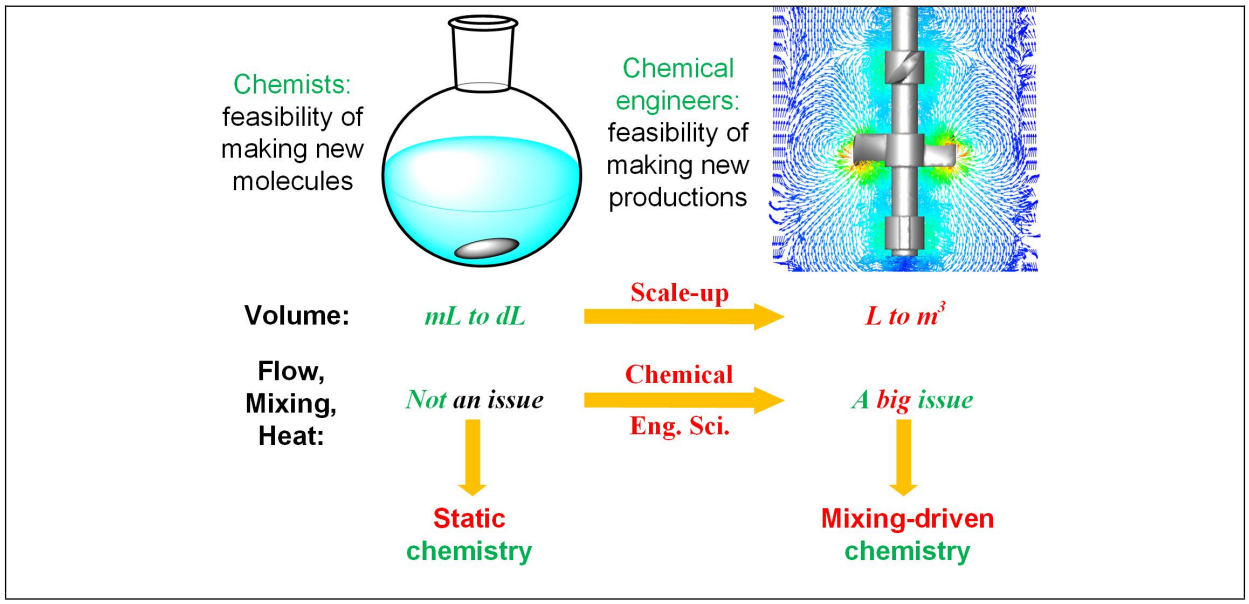

Figure 1. A simplistic vision of what chemists and chemical engineers do. Static chemistry versus mixing-driven chemistry.

Chemists and chemical engineers are key actors of chemical reactions. Nevertheless, their missions are not necessarily the same but complementary, as schematically depicted in Figure 1. Simply put, chemists study the feasibility of making new molecules and attempt to control the above three intrinsic kinetic parameters by tuning the molecular characteristics and/or developing catalysts. Therefore, they may only need to use a small reactor (milliliters to hundreds milliliters) and often a batch one so that flow field, mass transfer and heat transfer are not of concern. Chemical reactions conducted under such conditions may be called "*static chemistry*". On the other hand, chemical engineers study the feasibility of making new productions at an industrial scale. Therefore, they may have to use or develop large reactors (liters to dozens of cubic meters) which are more and more continuous ones. Among big challenges chemical engineers face with a big reactor are difficulties in efficiently homogenizing both the concentrations and temperatures of reactants over the entire reactor during the course of chemical reaction. In other words, mixing (three dimensional flow) and/or heat transfer now may become a big concern [1]. Chemical reactions conducted under such conditions may be called "*mixing-driven chemistry*". Over the last 15 year or so, chemists and chemical engineers also develop so-called "*flow chemistry*". It aims to better control key reaction conditions such as mixing, heat and temperature in order to selectively control the reaction pathways by continuously pumping reagents through a continuous micro-

reactor (high surface-to-volume ratio) or several ones in series, and continuously collecting the product [2,3]. In short, in the case of static chemistry, reaction conditions including the reactor itself are so chosen that mixing should not be of concern, whereas in the case of mixing-driven chemistry or flow chemistry, mixing is so optimized that the concentrations and temperatures of molecules are efficiently homogenized over the entire reactor.

A question then arises of whether or not flow or mixing could influence the three intrinsic kinetic parameters of Equation 1. Two scenarios may be envisioned, as shown in Figure 2. Scenario 1 is that flow or mixing is absent or is not strong enough to perturb the conformation and/or random rotation and movement of (statistically) spherical molecules in the entire reactor. This is often the case for small molecules (compared to polymers). Their relaxation time τ would be of the order of 10^{-7} to 10^{-10}s or their relaxation frequency ($f_{molecule}$) would be of the order of 10^{7} to 10^{10}Hz which is several orders of magnitude higher than the frequency of an agitator commonly used for mixing ($f_{agitator}$) which is of the order of 10^{1} to 10^{3}Hz. Since neither the conformation nor the random rotation/movement of the molecules is perturbed, mixing (3D flow) is not expected to have any noticeable effects on the intrinsic kinetic parameters. For this reason, one does not have to think about the effect of mixing on reaction kinetics unless it is controlled by advection and/or heat transfer, which is not the primary subject of discussion in this paper.

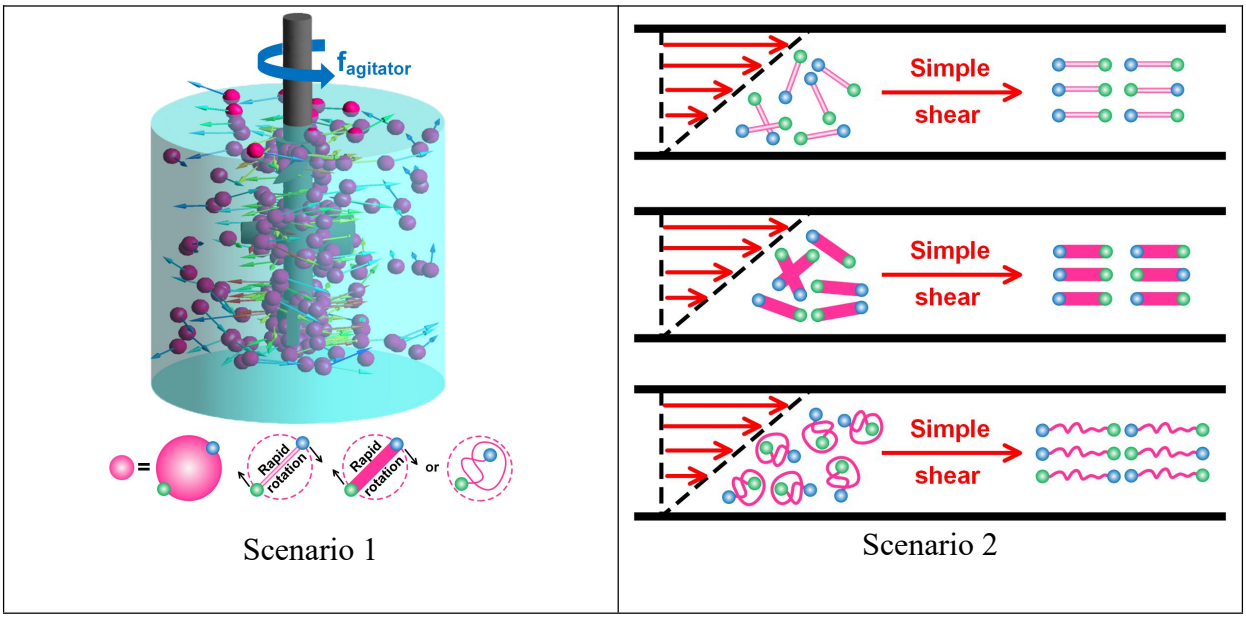

Figure 2: Scenario 1: molecules are in an equilibrium state, namely, they remain nearly or statistically spherical (under quiescent conditions or with a weak flow); scenario 2: molecules are in a non-equilibrium state, namely, they are permanently stretched and/or aligned by a strong unidirectional flow.

Scenario 2 is that molecules are subjected to a strong unidirectional flow so that they are permanently stretched and/or aligned in the flow direction. Would the three intrinsic kinetic parameters (f_c, f_e and ΔE) under this non-equilibrium state be the same as those in an equilibrium state (scenario 1)? The answer is likely no. If so, specific flow may influence the three intrinsic kinetic parameters if it is sufficiently strong to drive molecules from an equilibrium state to a non-equilibrium state.

For this reason, this perspective paper aims to bring about "*flow-driven chemistry*". The central idea of flow-driven chemistry is to control the dynamics (stretching, alignment, diffusion and collision) of molecules through a specific flow field in order to tune the kinetics and selectivity of (bio-)chemical reactions (promoting desirable ones and curbing undesirable ones). The primary goal of a specific flow field is not mixing which aims to homogenize the concentrations and temperature of molecules over the entire reactor, but to control molecular dynamics. Thus, flow-driven chemistry is not mixing-driven chemistry nor flow chemistry.

2. POTENTIAL APPLICATIONS OF FLOW-DRIVEN CHEMISTRY

As mentioned above, flow-driven chemistry aims to control reaction kinetics and/or selectivity through a specific flow field. An example of the application potentials of flow-driven chemistry is the growth versus cyclization of molecules which bear two complementary reactive groups. As shown in Figure 3, when one of the two complementary reactive groups of a molecule reacts with its complementary reactive group of another molecule, a molecule twice as long is formed - growth reaction. When the two complementary reactive groups of a given molecule react with each other, a ring molecule is then formed - cyclization reaction. For simplicity, assume that both the growth and cyclization reactions are irreversible and their rates are characterized by rate constants k_1 and k_2, respectively.

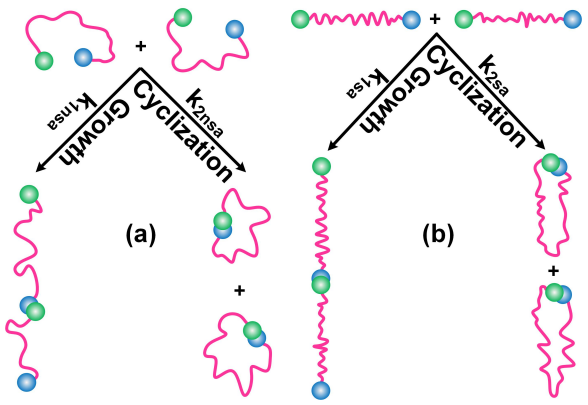

Figure 3. Growth and cyclization reactions of a molecule bearing two complementary reactive groups. (a) Molecules are in an equilibrium (under quiescent conditions or under a weak flow); (b) Molecules are in a non-equilibrium state (permanently stretched and aligned under a strong unidirectional flow).

Let us compare two cases: (3a) the reaction system is in an equilibrium state (under quiescent conditions or under a weak flow); (3b) molecules are in a non-equilibrium state (permanently stretched and aligned under a strong 1D flow). It is conceivable that the former is more favorable for the cyclization reaction than the latter, while it is exactly the opposite for the growth reaction. That is, $k_{1nsa}/k_{2nsa} < k_{1sa}/k_{2sa}$ where the subscripts "nsa" and "sa" denote "non-stretched and non-aligned molecules" and "stretched and aligned molecules". Thus, it is theoretically possible to control the selectivity of chemical reactions by controlling the stretching and/or alignment of reactive molecules through a specific flow field. Additionally, stretched and/or aligned molecules may diffuse faster, accelerating diffusion-controlled reaction kinetics and/or selectivity.

3. SCIENTIFIC BASES AND CHALLENGES OF FLOW-DRIVEN CHEMISTRY

The central scientific basis of flow-driven chemistry is to drive molecules from an equilibrium state to a non-equilibrium state (molecules are stretched and aligned) by a specific flow field. The degree of molecular stretching can be described by viscosity and/or radius of gyration of molecules, and that of molecular alignment by alignment angle. Figure 4 shows the effects of the simple shear rate on the kinematic viscosity (ν) which is the ratio between the dynamic viscosity and density (η/ρ), the radius of gyration squared (R_g^2) and the alignment angle (θ) of three $C_{30}H_{62}$ alkane isomers as examples [4]. A common feature is that for each of these three $C_{30}H_{62}$ isomers at a given temperature, there is a critical shear rate ($\dot{\gamma}_{cr}$) above which all the above three parameters start to vary. The critical shear rate is of the order of 10^8 to 10^9 s^{-1}. Specifically, when $\dot{\gamma} < \dot{\gamma}_c$, both ν (Figure 4a) and R_g^2 (Figure 4b) remain constant (first Newtonian region). This is because under this condition, the Deborah number *De* which is defined as $\tau\dot{\gamma}$ for a simple shear flow is smaller than unity ($De < 1$), indicating that flow is not strong enough to perturb the conformation of molecules in a sufficiently rapid manner so that they do not have enough time to relax themselves to their unperturbed state. Interestingly, θ keeps decreasing with increasing $\dot{\gamma}$ (Figure 4c), indicating that molecules are already aligned at $\dot{\gamma} < \dot{\gamma}_c$, even though they are individually still in an equilibrium state. When $\dot{\gamma} >$

$\dot{\gamma}_c$ or $De > 1$, ν starts decreasing (shear thinning region) with increasing $\dot{\gamma}$, and R_g^2 also starts varying (increasing and then going through a maximum or constantly decreasing), depending on the molecular architecture of the $C_{30}H_{62}$ isomer. As for θ, it starts leveling off with increasing $\dot{\gamma}$ and ultimately approaches limiting values between 6 and 11°. As expected, a more linear molecule or a molecule with a longer backbone (n-triacontane) has a smaller alignment angle θ or a higher degree of alignment.

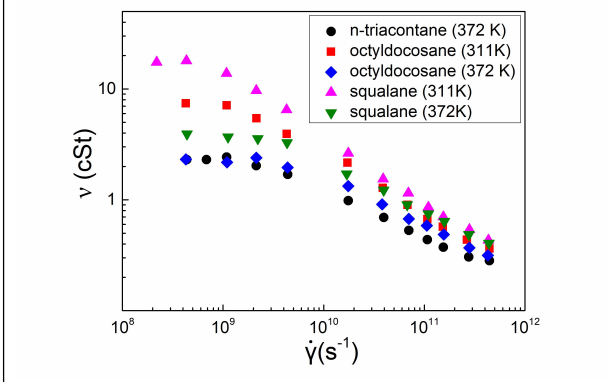

(a)

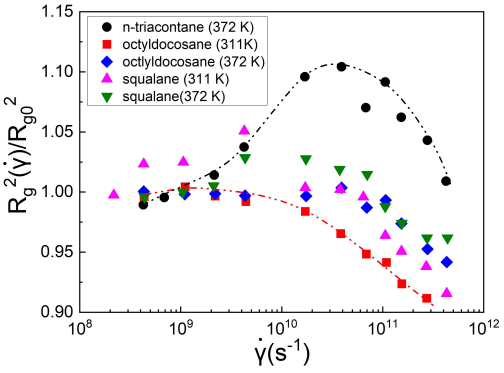

(b)

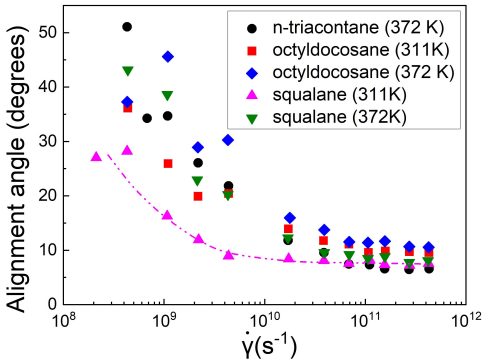

(c)

Figure 4: Effects of shear rate on he kinematic viscosity ν (a), radius of gyration squared R_g^2 (b), and alignment angle θ (c) of three $C_{30}H_{62}$ alkane isomers. The dashed curves are drawn to guide the eye. Adapted from Moore et al. [4].

Additionally, flow may also modify molecular diffusion coefficient when it has influenced the structural order (conformation and/or alignment) of the molecules. Figure 5 shows the effect of the rates of deformation of two types of 1D flows (planar Couette flow and planar extensional flow) characterized by the second scalar invariant II on the diffusion coefficients of three linear alkanes: $C_{20}H_{42}$, $C_{50}H_{102}$ and $C_{100}H_{202}$ [5]. II is proportional to the rate of energy dissipation ($2\dot{\gamma}^2$ for planar Couette flow, and $8\dot{\epsilon}^2$ for planar extensional flow). For both types of 1D flows, the diffusion coefficient significantly increases with increasing II, reaches a maximum (which is observed for $C_{20}H_{42}$ - the shortest molecule and not observed yet for $C_{100}H_{202}$ - the longest molecule within the computed range of II in the case of the simple shear flow, and is observed for all the three molecules in the extensional flow), and

then decreases with further increasing II. Moreover, the diffusion coefficient is more sensitive to II for planar extensional flow than planar Couette type.

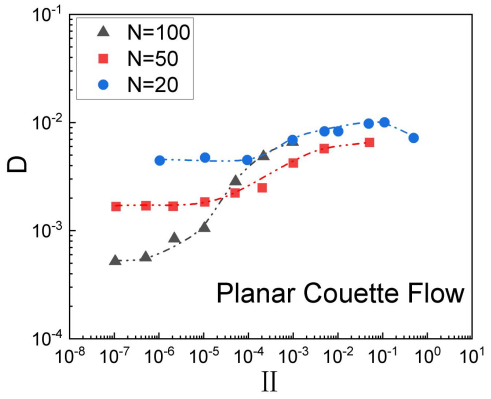

(a)

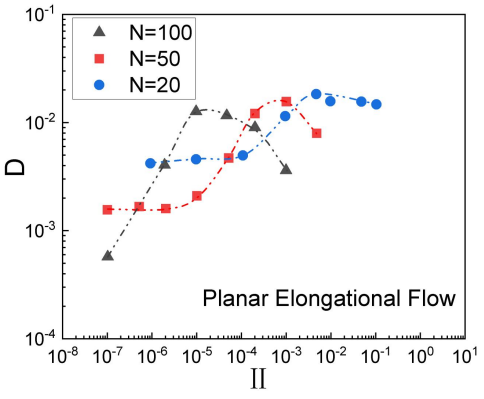

(b)

Figure 5: Effect of the second scalar invariant on the diffusion coefficient of linear alkanes C_NH_{2N+2}. (a) $II = 2\dot{\gamma}^2$ (planar Couette flow), (b) $II = 8\dot{\epsilon}^2$ (planar extensional flow). Circles: N = 20, squares: N = 50, and triangle: N = 100. The dashed curves are drawn to guide the eye. Adapted from Hunt et Todd [5].

A key scientific challenge is how to predict critical (shear) rate $\dot{\gamma}_{cr}$ necessary for significantly perturbing the conformation of molecules so that they are sufficiently far from their equilibrium state. When data of the dynamic viscosity $\eta(\dot{\gamma})$ as a function of shear rate $\dot{\gamma}$ are available, one may use Carreau-Yasuda model [6,7] to determine $\dot{\gamma}_c$ if it fits the data well. This model is given by Equation 2:

$$\eta(\dot{\gamma}) = \eta_\infty + \left(\eta_0 - \eta_\infty\right)[1 + (\dot{\gamma}/\dot{\gamma}_c)^\alpha]^{(n-1)/\alpha} \qquad (2)$$

where η_0 is the viscosity of the first Newtonian plateau (at very low shear rates), η_∞ is the viscosity of the second Newtonian plateau (at very high shear rates), α characterizes the smoothness of the transition of the viscosity from the first Newtonian plateau to the shear thinning regime, and n is the shear-thinning index.

For non-entangled molecules, when their η_0 and molar mass (M) are known, Einstein-Debye equation can be used to predict $\dot{\gamma}_c$. It is given by Equation 3:

$$\dot{\gamma}_c = \frac{\rho RT}{\eta_0 M} \qquad (3)$$

This equation is shown to work fairly well for low molecular weight alkanes [8] and not so for branched or entangled ones [9].

Molecular dynamics are also described by the Rouse model for non-entangled linear molecules [10-11] and by the reptation model for entangled ones [11-13]. The longest Rouse relaxation time (τ_R) and the longest reptation time (τ_d) are given by Equations 4 and 5 [11], respectively.

$$\tau_R = \frac{\zeta b^2}{3\pi^2 k_B T} \mathrm{N}^2 \sim \mathrm{M}^2 \qquad (4a)$$

$$\tau_d = \frac{\zeta b^4}{\pi^2 a_t^2 k_B T} N^3 \sim M^3 \qquad (4b)$$

Where ζ, b and N are the friction coefficient, the length and the number of a Kuhn monomer, respectively; k_B is the Boltzmann constant; a_t is the tube diameter; M is the molar mass of the molecule. One notices that $\tau_R \sim \mathrm{N}^2$ or M^2, and $\tau_d \sim \mathrm{N}^3$ or M^3.

In the Rouse model, the (dynamic) viscosity η_R is given by Equation (5a) [11]. Integration of Equation (4b) and (5a) yields Equation (5b) which indicates that $\tau_R \sim \eta_R^2$.

$$\eta_R \approx \frac{\zeta N}{b} \qquad (5a)$$

$$\tau_R = \frac{b^4}{3\pi^2 \zeta k_B T} \eta_R^2 \sim \eta_R^2 \qquad (5b)$$

In the reptation model, the (dynamic) viscosity η_d is given by Equation (6) which shows that $\tau_d \sim \eta_d$.

$$\eta_d \cong \frac{\pi^2 \rho R T}{12 M} \frac{\mathrm{N} b^2}{a_t^2} \tau_d \sim \tau_d \qquad (6)$$

From Equations (5b) and (6), one has:

For non-entangled molecules:	$\dot{\gamma}_c \sim \tau_R^{-1} \sim \eta_R^{-2}$	(7a)
For entangled molecules:	$\dot{\gamma}_c \sim \tau_d^{-1} \sim \eta_d^{-1}$	(7b)

Molecular dynamics simulations are gaining importance in predicting the structural order and transport properties of fluids including $\dot{\gamma}_c$. Figure 6 compares a molecular dynamics simulation method with the Einstein-Debye relation in terms of $\dot{\gamma}_{cr}$ for poly(α-1-decene) [14]. These two methods agree well for small molecules (the number of 1-decene n < 21). For large molecules (n > 21), differences between these two methods become significant, likely due to the ellipsoid shape assumption made in the Einstein-Debye equation [14]. The data produced by the molecular dynamics simulation method gives the following correlations:

$$\dot{\gamma}_c = 10^{16.252} M^{-2.444} \text{ for } 0 < \text{M} < 1895 \text{ g/mol} \quad (8a)$$

$$\dot{\gamma}_c = 10^{35.308} M^{-8.258} \text{ for } 1895 < \text{M} < 5000 \text{ g/mol} \quad (8b)$$

The exponent of M is -2.444 for the non-entangled molecules, which is slightly stronger than -2 predicted by the Rouse model (Equation 4a). It is -8.258 for the entangled molecules, which is much stronger than -3 predicted by the reptation model (Equation 4b). The branched structure of the poly(α-1-decene) is likely responsible for this discrepancy.

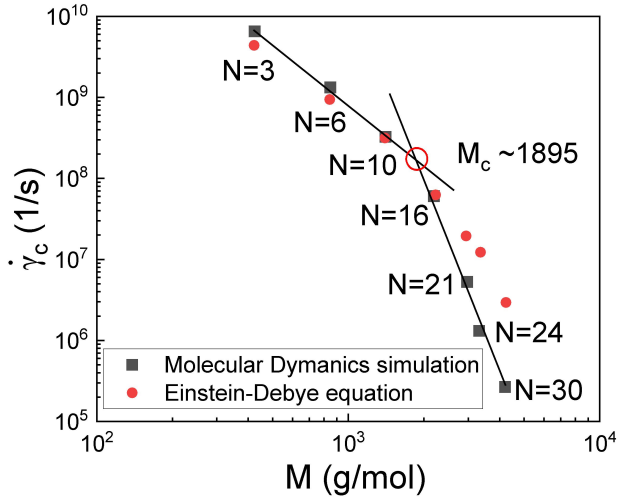

Figure 6: Critical shear rate as a function of the molar mass (M) of poly(α-1-decene) at 100°C calculated by the molecular dynamics simulations and the Einstein-Debye equation. N is the number of 1-decene in poly(1-decene). Adapted from Liu et al. [14].

The theories and models described above together with molecular dynamics simulations allow understanding and predicting, to some extent, the dynamics of molecules in an equilibrium state (without flow or with a weak flow: *De* <1) and the critical (shear rate) that would be necessary for driving the molecules to a non-equilibrium state (stretched and/or aligned under a strong flow: *De* >1). However, dynamics of molecules in a non-equilibrium state are poorly understood. Moreover, attention is yet to be paid to the effects of flow on the frequency, direction and energy of collisions between molecules which dictate the intrinsic reaction kinetics (Equation 1).

4. TECHNICAL BASES AND CHALLENGES

Technically speaking, flow-driven chemistry replies on methods of creating 1D flow in order to permanently stretching and/or aligning molecules. This requires that the rate of planar deformation be higher than the rate of relaxation of molecules (*De* > 1), and that flow be

laminar. While it is relatively easy to simultaneously meet these two requirements for entangled molecules such as polymers, it becomes very challenging for small chemical compounds. This is because the relaxation time of the latter would be on the order of 10^{-10} to 10^{-7} s. This would require a deformation rate of 10^{7} to 10^{10} s^{-1} while the Reynolds number should still be sufficiently small (< 2100 in a tube) so that the flow is laminar.

To show how challenging it can be to use a 1D flow to permanently stretch small molecules, let us take the example of the Poiseuille flow of a Newtonian fluid in a circular tube. The radius, diameter and length of the tube are designated by R, d and l, respectively; the dynamic viscosity and mass density of the fluid are designated by η and ρ, respectively; the velocity profile, average velocity and the pressure gradient of the flow are designated by $u(r)$, $\overline{u}$ and dp/dl, respectively. The u(r), $\overline{u}$, shear rate at the tube wall $\dot{\gamma}$ and Reynolds number Re are expressed by equations (8a-8f), respectively:

$$u(r) = -\frac{R^2}{4\eta}\frac{dp}{dl}\left[1-\left(\frac{r}{R}\right)^2\right]$$	(8a)
$$\overline{u} = \frac{R^2}{8\eta}\frac{dp}{dl}$$	(8b)
$$\dot{\gamma} = \frac{8\overline{u}}{d}$$	(8c)
$$Re = \frac{\rho\overline{u}d}{\eta}$$	(8d)

Based on equations (8b-8d), one obtains:

$$d = \left(\frac{8\eta Re}{\rho\dot{\gamma}}\right)^{1/2}$$	(8e)
$$\frac{dp}{dl} = \frac{32\eta\overline{u}}{d^2} = \frac{\dot{\gamma}^2\rho d}{2Re}$$	(8f)

Denote $\dot{\gamma}_c$ as the critical shear rate which is necessary for permanently stretching a molecule. Consider a hypothetical fluid whose ρ is $1x10^3$ $kg.m^{-3}$ and suppose that when η is 0.1 Pa.s, $\dot{\gamma}_c$ is $1x10^8$ s^{-1}. When η is 1 or 10Pa.s, the corresponding $\dot{\gamma}_c$ is scaled to $1x10^6$ or $1x10^4$ s^{-1} using the scaling law $\dot{\gamma}_c \sim \eta^{-2}$ (Equation 7a for non-entangled molecules; experimentally $\dot{\gamma}_c \sim \eta^{-1.8}$[15]). The use of the above equations (8b-8f) allows calculating d, $\overline{u}$ and dp/dl as a function of $\dot{\gamma}_c$ for various values of η and Re = 2100 to ensure laminar flow. The calculated values are shown in Table 1.

Table 1: Values of the tube diameter d, average velocity $\bar{u}$ and pressure gradient dp/dl for three pairs of viscosity η and critical shear rate at wall $\dot{\gamma}_c$ to permanently strech molecules under a laminar flow (Renolds number Re = 2100).

$\dot{\gamma}_c \sim \eta^{-2}$ ($\dot{\gamma}_c \sim \eta^{-1.8}$ [15])	d (µm)	$\bar{u}$ (m.s^{-1})	dp/dl (bar.m^{-1})
η = 0.1Pa.s, $\dot{\gamma}_c$ = 1x10^{8}s^{-1}	130	1625	3.08 x 10^6
η = 1Pa.s, $\dot{\gamma}_c$ = 1x10^{6}s^{-1}	410	512	9.76x10^2
η = 10Pa.s, $\dot{\gamma}_c$ = 1x10^{4}s^{-1}	1300	1.625	0.308

This table shows that the tube diameter should be smaller than 130µm in order that the shear rate at its wall reaches 1 x 10^{8}s^{-1} and that the flow is a laminar one. The corresponding average velocity is 1625m.s^{-1}, meaning that for a tube of 1625m long, the average residence time of the fluid in the tube is only 1s, which is extremely short. Even if 1s was long enough for a reaction, it would still be extremely difficult to make a tube of 130µm in diameter and 1625m in length. Moreover, even if one could make such a tube, it would not be able to stand the pressure gradient (3.08x10^{6}bar.m^{-1}). If η is increased from 0.1Pa.s to 1 or 10Pa.s, d = 410 or 1296µm, which is technically much more feasible. The corresponding $\bar{u}$ is 512 and 1.62m.s^{-1}, and dp/dl is 9.76 x 10^2 and 0.308bar.m^{-1}, respectively. The above approximate calculations show that the viscosity of a reaction system should be above 1Pa.s and preferably above 10Pa.s so that the critical shear rate required for permanently stretching molecules can be achieved in practice. Above this viscosity, the tube diameter will not have to be too long while the corresponding residence time will not be too short. This implies that for low-viscosity reaction systems, they may need to be viscosified. Considering the very high shear rate, viscous dissipation can also be an issue.

5. STATE OF THE ART OF THE UNDERSTANDING RELATED TO FLOW-DRIVEN CHEMISTRY

Molecules may need to be brought into contact by advection and/or molecular diffusion before they may collide with each other. Thus, conceptually the overall rate of a chemical reaction is controlled by at least one of the rates of three consecutive steps: advection, molecular diffusion and chemical reaction *per se*. There are numerous theoretical and experimental studies on mixing-driven chemistry: the effects of advection through mechanical mixing (3D flow) on the overall rate and/or selectivity of chemical reactions [1, 16-18]. By contrast, studies related to flow-driven chemistry are scarce and very fragmented. Indeed,

there are only a very few number of theoretical studies and an even fewer number of well-controlled experimental ones on the effects of 1D flow on diffusion-controlled reaction kinetics. Thus these studies are very precious for supporting the emergence of flow-driven chemistry. As such some of them are outlined below.

5.1. Theoretical developments

Thus far, the literature has only developed theories or models for the effects of 1D flow on the kinetics of three types of chemical reactions which occur irreversibly in a homogeneous liquid state and of which the rates are diffusion-controlled. There is no theoretical development for multiphase liquid systems. Figure 7 depicts these three types of reactions: intermolecular (coupling) reaction, intramolecular (cyclization) reaction and polymerization of rod-like molecules.

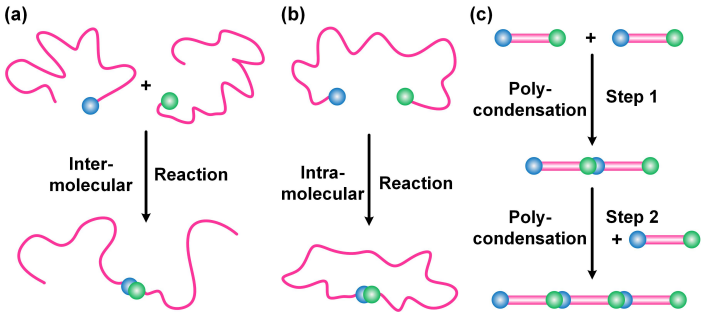

Figure 7. (a) An intermolecular (coupling) reaction; (b) an intramolecular (cyclization) reaction; (c) polycondensation between two rod-like bi-functional monomers.

5.1.1 Effects of 1D flow on diffusion-controlled reactions in homogeneous systems

A theoretical framework set up by De Gennes [19-20] for dense homogeneous polymer systems under quiescent conditions is a relevant starting point to address the effects of flow. Fredrickson and Leibler included the effect of a steady linear flow in that framework for polymer systems in which a small fraction of the chains have a single, terminally attached reactive group that can react irreversibly with a second reactive group on a different chain - intermolecular (coupling) reaction [21]. In the case of a weak flow ($De \ll 1$), the relationships between the reaction rate constant k and De for a simple shear flow and an uni-axial extensional flow are given by Equations 9a and 9b:

For a simple shear flow:	$k_{shear} = 50.26 D_0 R(1 + 0.8068 De^{1/2} + \ldots)$ for $De \ll 1$	(9a)
For a uni-axial extensional flow:	$k_{elong} = 50.26 D_0 R(1 + 1.258 De^{1/2} + \ldots)$ for $De \ll 1$	(9b)

where R is the radius of gyration of the chain, and D_0 is the (reactive) chain center-of-mass diffusion coefficient and De are defined by Equations 10a-10b for non-entangled and entangled chains, respectively. Equations 9a-9b show that even if molecules are not fully stretched ($De << 1$), both simple flow and uni-axial extensional flow already accelerate the rate of a diffusion-controlled irreversible intermolecular (coupling) reaction. Moreover, a uni-axial extensional flow is more effective than a simple shear flow at accelerating the rate of such a reaction.

For a non-entangled polymer system	$D_0 = \frac{k_B T}{N\zeta}$ $De = \beta\tau_R$	(10a1) (10a2)
For an entangled polymer system:	$D_0 = \frac{k_B T a_t^2}{3N^2\zeta b^2}$ $De = \beta\tau_d$	(10b1) (10b2)

where β is the the flow strength (shear or extensional rate).

In the case of a strong shear flow ($De >> 1$), the relationships between the reaction rate contant k and De are given by Equations 9a and 9b:

For a non-entangled polymer system	$k_{shear} \approx 52.908 D_0 R De^{1/3} \sim \dot{\gamma}^{1/3}$ for $De \to \infty$	(11a)
For an entangled polymer system:	$k_{shear} \approx 32.234 D_0 R \frac{De}{lnDe} \sim \frac{\dot{\gamma}}{ln\dot{\gamma}}$ for $1 \ll De \ll \tau_d/\tau_R \sim N$ $k_{shear} \sim \dot{\gamma}^{1/3}$ for $De \gg \tau_d/\tau_e \sim N^3$	(11b1) (11b2)

Where $\tau_e \approx a_t^4\zeta/k_B T b^2 \ll \tau_R \ll \tau_d$ is the time for a Rouse displacement of the order of the the tube diameter to occur [11]. Equations 11a-11b1 show that k_{shear} of an entangled polymer system is much more sensitive to the shear rate than a non-entangled one, unless De becomes very high, $\gg \tau_d/\tau_e \sim N^3$(Equation 11b2).

Fredrickson et al. extended the above theoretical framework for irreversible and diffusion-controlled inetrmolecular (coupling) reactions to irreversible and diffusion-controlled intramolecular (cyclization) reactions under flow [22]. More specifically, relatively low molar mass Rouse chains, each bearing two complementary reactive groups at their chain ends, are dispersed in a melt of unfunctionalized, but otherwise identical, chains. The cyclization reaction occurs instantaneously and irreversibly when the two terminal

complementary reactive groups of a reactive chain approach to within a "capture radius" (the order of a monomer size) of each other. The relationships between the cyclization rate constant k and De are given below:

For simple shear flow:	$k_{shear} \approx \frac{0.46}{\tau_R}(1 - 0.18De^2)$ for $De \ll 1$ $k_{shear} \approx \frac{0.38}{\tau_R} De^{-2/3} \sim \dot{\gamma}^{-2/3}\, \mathrm{N}^{-10/3}$ for $De \gg 1$	(12a1) (12a2)
For uniaxial extensional flow:	$k_{elong} \approx \frac{0.46}{\tau_R}(1 - 0.76De^2)$ for $De \ll 1$	(12b)

Comparison between Equations 12a1 and 12b shows that a uni-axial extensional flow is more effective than a simple shear flow at reducing the rate of a diffusion-controlled irreversible intramolecular reaction (cyclization reaction), due to the larger stretching of the molecules in the extensional flow. Inspection of Equations 9a and 12a1 shows that the positive effect of a weak simple shear flow (De << 1) on the rate of a diffusion-controlled irreversible intermolecular (coupling) reaction is more pronounced than its negative effect on the rate of a diffusion-controlled irreversible intramolecular (cyclization) reaction, $+0.8068De^{1/2}$ versus $-0.18De^2$ for the first flow correction. By contrast, in the case of a strong simple shear flow (De >>1), its positive effect on the rate of a diffusion-controlled irreversible intermolecular reaction is smaller than its negative effect on that of a diffusion-controlled irreversible intramolecular reaction ($De^{1/3}$ versus $De^{-2/3}$). These results can be industrially relevant.

5.1.2 Effects of uni-directional flow on diffusion-controlled polymerizations in homogeneous systems

Khakhar et al. developed a model for flow-enhanced diffusion-controlled polycondensation of rod-like molecules [23]. Any two molecules with appropriate terminal reactive groups may react to form a larger one. They consider that reaction requires translation of the two reacting rods so that the terminal reactive groups are within a critical reaction radius a as well as rotation so that the parallel relative orientation of the rods reaches below a critical one: $\theta < \theta c$. This is depicted in Figure 8. The reaction becomes diffusion-controlled with an increase in the length of the rods during the polymerization due to reduced mobility. The mobility of rods is expressed in terms of three diffusion coefficients: $D_{\parallel}$, the translational diffusivity parallel to the rod axis; $D_{\perp}$, the translational diffusivity perpendicular to the rod axis; and D_r, the anisotropic rotational diffusivity. The flow strength to which the

polymerization system is subjected is characterized by the ratio between the extensional rate and rotational diffusivity, ε/D_r, and the effect of flow on the rate of reaction is characterized by the relative reaction rate constant k_{eff}/k_{int}, with k_{eff} being the effective reaction rate constant and k_{int} the intrinsic reaction rate constant in the absence of diffusional limitations and flow.

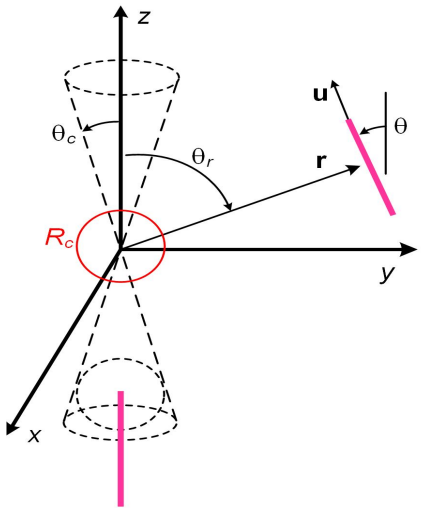

Figure 8. Schematic diagram showing the criteria for reaction between rod-like molecules. Molecules can react only if they are in a capture radius *Rc* of each other and their relative orientation angle θ is smaller than a critical value θ_c.

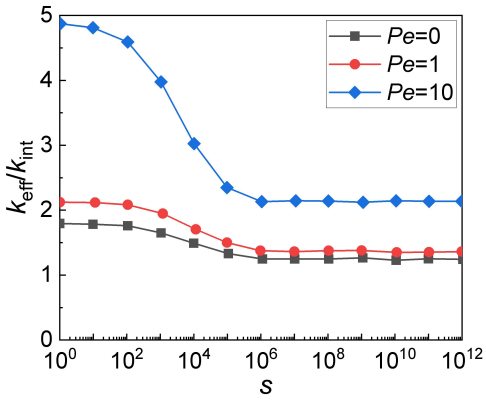

Figure 9. Variation of k_{eff}/k_{int}, the ratio between the effective reaction rate constant (k_{eff}) and the intrinsic one (k_{int}) without diffusion limitations nor flow, for different flow strengths (ε/D_r). $\delta = k_{int}/[4\pi a(1-\cos\theta_c)D_{\parallel}] = 1$, $D_{\perp}/D_{\parallel} = 0.01$, and $\theta_c = 0.01$.

Figure 9 shows the variation of the relative rate constant k_{eff}/k_{int} as a function of the rotational diffusional resistance $s = D_{\parallel}/a^2 D_r$ for different flow strengths (ε/D_r). The k_{eff}/k_{int} increases with increasing ε/D_r. In the case of no flow ($\varepsilon/D_r = 0$) and high rotational diffusivity (small s), the effective rate constant is equal to the intrinsic rate constant, namely $k_{eff}/k_{int} = 1$, as expected. Surprisingly, increasing flow strength increases the relative rate constant to values even greater than unity, implying that the effective rate of reaction is higher than the intrinsic rate of reaction. This may be explained by the flow-driven orientation and alignment of molecules which result in a higher effective collision frequency of molecules ($f_e f_d$ of Equation 1) suitable for reaction.

5.1.3 Mechano-chemistry

At this point, it is worth-mentioning mechanochemistry which has regained interests in recent years due to its unnecessity of using solvents for reaction [24]. The central idea of

mechanochemistry is to use an external force (F) to deform bonds of molecules in order to reduce the activation energy (ΔE) necessary for breaking bonds. A phenomenological description of the reaction rate constant k for breaking a bond is given by the following equation [25, 26]:

$$k = \omega \frac{k_B T}{h} e^{-(\Delta E - \Delta x F)/k_B T} \quad (13)$$

where h is the Planck constant, ω is the transmission coefficient; and Δx is viewed as the difference along the force vector in the distance of the molecule between its ground- and transition-state geometries, although it may not necessarily have a geometrical meaning. In a first approximation, Δx is given by the following equation:

$$\Delta x = k_B T \frac{\partial ln k}{\partial F} \quad (14)$$

Equation 12 shows that the activation energy ΔE is reduced by a factor $\Delta x F$ when a molecule is subjected to an external force F, increasing therefore the reaction rate constant k. Flow generates forces and therefore is expected to reduce the activation energy ΔE.

The ratio $\Delta x F / \Delta E$ characterizes the relative contribution of an external force F to the reduction in ΔE. Consider a molecule which is subjected to a simple shear flow with a shear stress τ_{shear}. Assuming that under the flow, the molecule be in a cylindrical shape with a diameter d_s. The force to which it is subjected $F_s = \frac{\pi}{4} d_s^2 \tau_{shear} = \frac{\pi}{4} d_s^2 \eta \dot{\gamma}$. Denote ΔE_s as the activation energy necessary for breaking a single bond. Take $d_s \sim 1nm$, $\eta \sim 0.1 Pa.s$, $\dot{\gamma} \sim 1\text{x}10^8 s^{-1}$(of the order of a critical shear rate for permanently stretching a small molecule), and $\Delta x \sim 0.1nm$ [27]. Then the ratio $\Delta x F_s / \Delta E_s$ for breaking a bond of a single molecule is of the order of 5% or 1% if the activation energy ΔE is taken as $1\text{x}10^4$ or $5\text{x}10^4$J/mol. This numerical analysis indicates that for many types of chemical reactions, the contribution of flow to their activation energy ($\Delta E \sim 1\text{x}10^4$ to $5\text{x}10^4$ J/mol) is negligible, even if the flow is very strong ($\tau_{shear} \sim 1\text{x}10^7 Pa$).

5.1.4 Effects of flow on chemical reaction equilibra

A flow raises the Gibbs free energy of a chemical reaction system [28]. As a consequence, the chemical equilibrium is modified by a factor which is proportional to $\dot{\gamma}^2$ [28]. Under a very strong flow ($\tau_{shear} \sim 1\text{x}10^7 Pa$ or higher for example), its influence on the chemical equilibrium constant might become significant.

5.2 Experimental observations

The literature is poor in terms of the experimental study of the effect of a unidirectional flow on the rates of chemical reactions. Very often, the flow pattern is so complicated that it is difficult to discriminate between the effects of mixing (3D flow) and those of 1D flow. To the best of the author's knowledge, there are only a very few relevant experimental works [29, 30] on intermolecular (coupling) reactions (Figure 7a) in a homogeneous liquid state, but none on intramolecular (cyclization) ones (Figure 7b). There are only two relevant works on polymerization (Figure 7c) [31, 32]. After all, this is not surprising for the reasons presented in section 4 concerning technical challenges of flow-driven chemistry. A lack of awareness of potential scientific and technical interests would also be a reason. It is worth-mentioning two well-controlled experimental studies on the effect of mixing and/or a unidirectional flow on the kinetics of interfacial reactions between complementary reactive groups attached to the ends of two immiscible polymer chains [33-37].

5.2.1 Effects of mixing/flow on intermolecular (coupling) reactions in homogeneous systems

Branching of a high density polyethylene with a melt flow index of 8g/10min (190°C, 2.16 kg) by dicumyl peroxide is studied in an internal mixer which has a chamber in the form of 8 [29]. Two rotors in this chamber rotate at different rates in opposite directions to ensure mixing. The branching corresponds to the recombination between two radicals attached to two polyethylene chains. The following relationships are established between the average branching (recombination) rate constant k_{rc} and average *De (* the reptation relaxation time t_d is determined to be 0.17s, and *De* varies between 0.88 and 4.4):

In the lower range of De	$k_{rc} = 0.0147(1 + 2.372De^{0.44})$	(15a)
In the higher range of De	$k_{rc} = 0.0275\frac{De}{lnD}$	(15b)

Equations 15a-15b are more or less in agreement with Fredrickson and Leibler's model (Equations 9a-11b1), despite the complexities in terms of the reaction system, the architecture of branched polymer chains and the flow field. Given these complexities it would be presumptuous to conclude that this study irrevocably validates or not Fredrickson and Leibler's model.

Stress within the human circulatory system is known to alter the signaling pathways of endothelial cells via a mechanosensory complex. Hakala et al. [30] use an artificial capillary

system of a few dozens of micrometers in diameter to study the effect of shear stress generated by a simple shear flow on the rate with which the reactive thiolate form of a protein such as Cys34 is trapped by 4-fluoro-7-sulfamoylbenzofurazan, an electrophilic fluorogenic dye. The shear stress in the capillary is increased by decreasing the capillary diameter and/or increasing flow rate. Figure 10 shows that the trapping rate increases almost linearly with increasing shear stress which deforms the protein to trigger a conformational change so that it becomes more accessible to solvent.

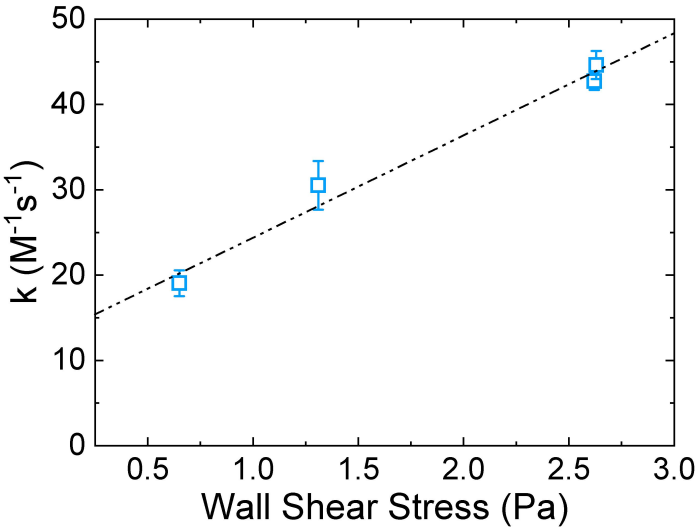

Figure 10. An increase in the pseudo-first-order rate constant of the trapping of a protein (Cys34) by 4-fluoro-7-sulfamoylbenzofurazan with increasing shear stress in an artificial capillary system to mimic the human circulatory system. Adapted from Hakala et al. [30].

5.2.2 Effects of mixing/flow on polymerizations in homogeneous systems

The effect of a simple shear flow on the rate of polymerization experimentally shown by Khakhar et al. using a Couette flow in coaxial cylinders as a reactor [31]. The polymerization involves the polycondensation between two rod-like bi-functional monomers, as shown in Figure 11a. Figure 11b shows the increase in the weight average degree of polymerization $\overline{DP}_w$with polymerization time in reactor I with a 3D flow (mixing) and reactor II with a simple shear flow of various flow strengths. The $\overline{DP}_w$ increases faster in the initial stage of the polymerization than in the late stage of the polymerization, suggesting that the rate of polymerization is likely controlled by the intrinsic reaction kinetics in the initial stage and becomes diffusion-controlled in the late stage. Moreover, in the late stage of the

polycondensation, the $\overline{DP}_w$ is significantly higher in reactor II than in reactor I, and the difference is even more significant at a higher shear rate.

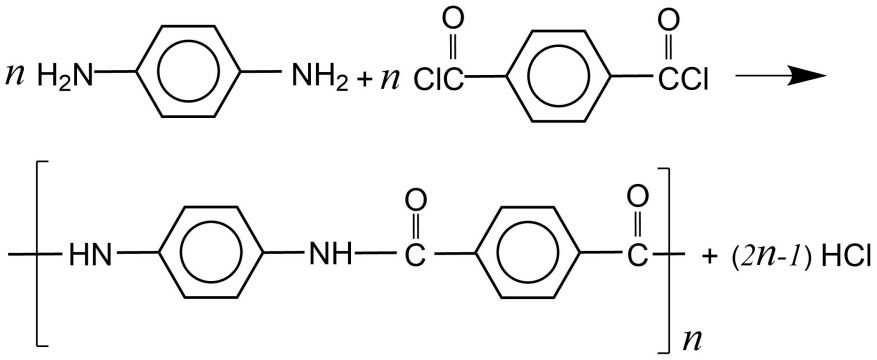

(a)

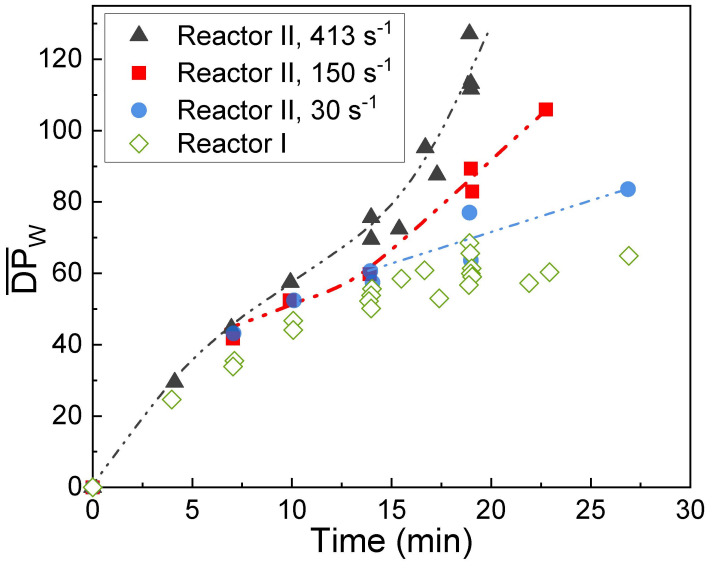

(b)

Figure 11. (a) Polycondensation reaction between two rod-like bi-functional monomers; (b) increase in the weight average degree of polymerization ($\overline{DP}_w$) of the polymer obtained in reactor I with mixing (3D flow) and reactor II with various simple shear rates. The dashed curves are drawn to guide the eye. Adapted from Khakhar et al. [31].

One may argue that this is due to an improved mixing. To check this, the polycondensation reaction is conducted in reactor II at the same total strain and polymerization time but for two different shearing histories: for experiment 1, $30s^{-1}$ for 1 to 7min, $413s^{-1}$ for 7-13min and $413s^{-1}$ for 13-19min; for experiment 2, $413s^{-1}$ for 1 to 7min,

413s^{-1} for 7-13min and 30s^{-1} for 13-19min. The resulting $\overline{DP}_w$is 113 for experiment 1 and only 63 for experimental 2. These results confirm that it is not so useful to strongly shear the polymerization system at the initial stage of polymerization where the polymerization rate is reaction-controlled, but crucial to do so in the late stage of polymerization where the rotational diffusion and therefore the orientation of the rod-like molecules to within a critical relative orientation angle (θ_c) are slow (Figure 11a). Since molecular orientation (1D flow), rather than mixing (3D flow), is responsible for the higher polymerization rate during the slow, diffusion-controlled phase of polymerization, the geometry of the reactor for this stage should allow promote a 1D flow in order to promote molecular alignment. For example, an annular geometry or a tube to produce a simple shear flow with a sufficiently high shear rate could suffice for the late stage of the polymerization instead of complex designs that are used in practice which promote mixing (3D flow).

The above work is elegant but suffers from a flaw: it uses a polycondensation reaction which yields a small molecule (HCl in this work). The latter may need to be thoroughly removed in order to obtain a sufficiently high degree of polymerization, especially in the late stage of polymerization. The removal of this small molecule becomes more difficult in the late stage of polymerization due to higher viscosity, requiring more efficient mixing. Therefore, it is not easy to discriminate the effect of mixing on the removal of the small molecule and that of simple shearing on the orientation of reactive molecules. Zhang et al.'s work [32] suffers from the same flaw.

5.2.3 Effects of mixing/flow on intermolecular (coupling) reactions in heterogeneous systems

Macosko et al. [33, 34] conducted well-controlled experiments to study the effect of flow and/or mixing on the kinetics of coupling reactions between immiscible reactive polymers using primarily an amine terminated polystyrene (PS-NH_2) and an anhydride terminated poly(methyl methacrylate) (PMMA-An) as model functional polymers. Reactions are done either under static conditions using PS-NH_2/PMMA-An bilayer flat films, or under mixing in a cup-rotor mixer with three steel balls (maximum shear rate: ~ 100s^{-1}). The reaction temperature is between 175 and 200°C. Table 2 compares the PS-NH_2/PMMA-An interfacial reaction rate constants under static and under mixing conditions [33, 34]. Those of homogeneous amine/anhydride (systems PS-NH_2/PS-An and PMMA-NH_2/PMMA-An) are shown as references [33, 35]. Two findings are striking: (a) the reaction rate constants of the heterogeneous systems (PS-NH_2/PMMA-An) under mixing are two to three orders of magnitude

higher than those under the static conditions; (b) they are of the same order of magnitude as those of the homogeneous analogues, if not higher.

Table 2. Second-order reaction rate constants of amine/anhydride heterogeneous and homogeneous reaction systems under static condition and/or under mixing. Data are taken from references [33-35].

	Polymer1/Polymer 2 Mn_1/Mn_2 (kg.mol^{-1})	k_{ci} (kg.mol^{-1}. min^{-1})
PS-NH_2/PMMA-An bilayer film under static condition	PS-NH_2/PMMA-An 17/15	12 at 200°C
	PS-NH_2/PMMA-An 18/12	15 at 175°C
	PS-NH_2/PMMA-An 26/15	3.2 at 175°C
Heterogeneous PS-NH_2/PMMA-An systems under mixing	PEE-NH_2/PS-An 18/35	1700 at 200°C
	PS-NH_2/PMMA-An (26+72/12*	950 at 180°C
	PS-NH_2/PMMA-An 15/12	4200 at 180°C
Homogeneous aromatic amine/anhydride systems under mixing	PS-NH_2/PMMA-An 26/15	5300 180°C
	PS-ArNH_2/PS-An 26.7/25.3	3.3 at 180°C
	PMMA-ArNH_2/PMMA-An 25.8/25.3	1.9 at 180°C
Homogeneous aliphatic amine/anhydride systems under mixing	PS-NH_2/PS-An 26.7/25.3	~ 1400 at 180°C
	PMMA-NH_2/PMMA-An 25.8/25.3	~ 10^3 at 180°C [35]
	PMMA-NH_2/PMMA-An 36/15	84 at 180°C [33]

*: The blend consisted of mixture of 18% 26 kg/mol PS-NH_2, 57% 72 kg/mol PS-NH_2, 10% PMMA-An, and 15% nonfunctional PMMA.

If the reaction rate constants of the heterogeneous functional polymer systems under mixing are indeed higher than those of their homogeneous analogues, then this suggests that they are even higher than intrinsic reaction rate constants without adverction and diffusion limitations. According to reference [33], these reactions are not diffusion-controlled. If so, this finding is one of the very few in support of flow-driven chemistry. Nevertheless, given the experimental errors involved, one cannot ascertain that the reaction rate constants of the heterogeneous functional polymer systems under mixing are indeed higher than those of their

homogeneous analogues. Moreover, the interfacial area generation in the cup-mixer is complex and it is difficult to isolate the effects of flow on reaction kinetics.

For this reason, a subsequent work [36] uses a multilayer co-extruder to fabricate a 640-layer polystyrene (PS)/poly(methyl methacrylate) (PMMA) sample. The PS and PMMA contain 10wt% PS-NH_2 and PMMA-An, respectively. The coupling interfacial reaction occurs between well-defined PS-NH_2 and PMMA-An layers during the co-extrusion. This study confirms the above finding that the coupling reaction under coextrusion is as rapid as that under mixing and is up to 1000 times faster than that under quiescent annealing. It speculates that the high surface energy of the functional chain ends causes them to be depleted near the interface, leading to very slow coupling under quiescent conditions and that the diffusion of polymer chains very close to the interface is much slower than in bulk [38]. Under coextrusion or mixing, external flow increases the functional group concentrations in the interfaces, restoring reaction rates to the level expected under homogeneous conditions. It further argues that extensional flow is more important than shear flow in accelerating the interfacial coupling reaction.

The above finding is corroborated by another work [37] which studies the rate of coupling reaction between a terminal amine group attached to polyamide 6 and anhydride groups attached randomly to a polyethylene backbone using bilayers prepared by coextrusion or lamination. Figure 12 shows that when all other parameters are kept constant, the reaction rate during coextrusion through a compressive die is almost two-orders of magnitude higher than that through a non-compressive die. The latter is close to that of quiescent lamination.

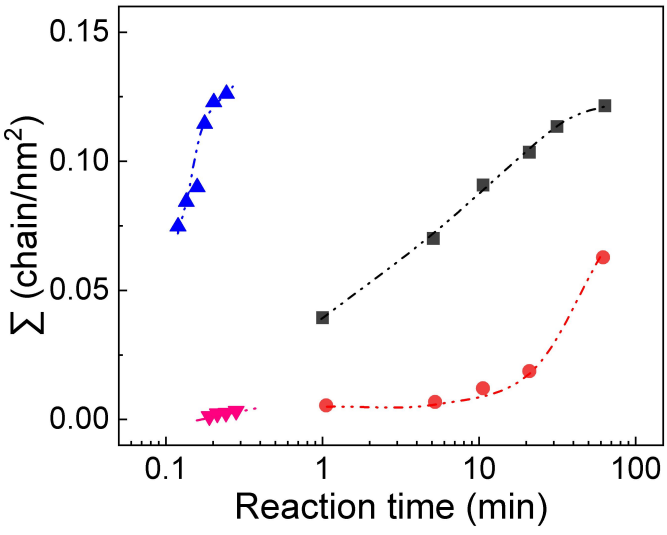

Figure 12. Interfacial copolymer density Σ vs. reaction time for the coupling reaction between the terminal amine of polyamide 6 and anhydride moieties attached randomly along a polyethylene backbone. Quiescent lamination at 230°C, quiescent lamination at 170°C, coextrusion with a non-compressive die at 230°C, coextrusion with a compressive die at 230°C. The dashed curves are drawn to guide the eye. Adapted from Song et al. [37].

5.2.4 Interfacial reactivity of functional groups

When two complementary functional groups A and B react with each other in a liquid state, textbooks [39] tell that their overall reaction rate constant does not exceed its intrinsic reaction rate constant, and that it reaches its upper bound (the intrinsic reaction rate constant) only when the reaction rate is not controlled by the rate of advection nor that of molecular diffusion but only by the effective collision frequency. Moreover, the longer the molecules which bear the complementary functional groups, the smaller the overall and/or intrinsic reaction rate constants. Thus, the reaction rate constants of functional groups attached to small molecules are considered as the upper bounds of those attached to polymers. Consider four hypothetical reaction systems which have the same volume and the same numbers of A and B functional groups (see Figure 13). In system (a), molecules bearing A and B functional groups are small and mutually miscible. System (b) differs from system (a) only in that the B functional group is attached to a polymer chain end. Nevertheless, they remain miscible. In system (c), both A and B functional groups are attached to polymer ends of the same chemical nature. The system is thus miscible. In system (d), A and B functional groups are attached to polymer ends of different chemical natures, which are immiscible. In other words, in the first three homogeneous systems, the A and B functional groups are randomly distributed over the entire reaction volume at the molecular scale. In the last heterogeneous system, given that A-bearing polymer and B-bearing polymer are immiscible, most of the A and B functional groups are located in their respective polymer phases. Only small fractions of them can be located in the interfaces where they may collide and react with each other.

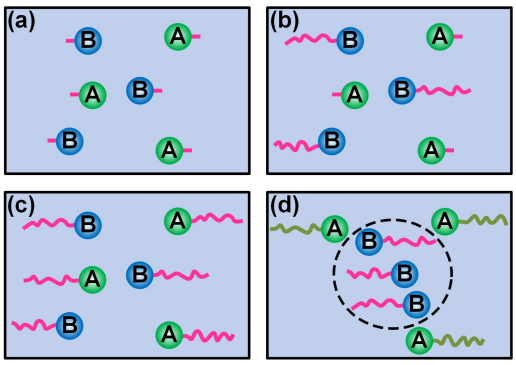

Figure 13. (a) A+B miscible system of A + B; (b) A + B– bearing polymer miscible system; (c) A-bearing polymer + B-bearing polymer miscible system; (d) A-bearing polymer + B-bearing polymer immiscible system. All four reaction systems have the same volume and contain the same numbers of A and B functional groups. Adapted from Feng and Hu [40].

Since the nominal molar concentrations of the complementary functional groups in the above four reaction systems are the same, according to textbooks one would rank their overall reaction rate constants in the following order: $d \ll c \leq b \leq a$. Feng and Hu show that under mixing, $d \gg b$ and speculate that the reactivity of functional groups attached to polymer chains confined at the interface to within a capture radius R_c is much higher than their small molecule analogues [40]. Specifically, a comparison is made between a heterogeneous reaction system (d) and a homogeneous one (b) based on the reaction between isocyanate and hydroxyl groups. The former is composed of a chemically inert polystyrene (PS), a terminal hydroxyl PS denoted as PS–CH_2CH_2–OH (Mn = 53.7 kg/mol) [41], a chemically inert poly(methyl methacrylate) (PMMA), and a random copolymer of MMA and 3-isopropenyl-α,α-dimethylbenzyl isocyanate), denoted as PMMA-r-NCO (Mn = 27.9 kg/mol; isocyanate bearing mononer content: 1.5%) [42, 43]. The homogeneous analogous reaction system consists of the PMMA, PMMA-r-NCO, and 3-phenyl 1-propanol (an analogue of PS–CH_2CH_2-OH denoted as Ph-$CH_2CH_2CH_2$-OH). An internal mixer is used to process these two reaction systems at a set temperature of 175°C upon following one of the three mixing modes: (a) continuous mixing at 64 or 84 rpm; (b) stepwise mixing alternating between 0 and 64 rpm; (c) no mixing except for the very first minute during which the rotors turn at 64 rpm to ensure the melting and a certain degree of homogenization of the reaction systems.

Figure 14 compares the (PMMA+PMMA-r-NCO)/(PS+PS-CH_2CH_2-OH) heterogeneous macromolecular alcohol reaction system with the (PMMA+PMMA-r-NCO)/Ph-$CH_2CH_2CH_2$-OH homogeneous small alcohol one in terms of the percentage of conversion of the NCO group as a function of time. A striking finding is that the conversion of the heterogeneous macromolecular alcohol system is always above the homogeneous small alcohol one, whatever the mixing mode. Specifically, in the case of the homogeneous small alcohol reaction system, the reaction proceeds continuously with time and its pace seems to be the same for all three mixing modes. By contrast, the situation is very different for the heterogeneous macromolecular alcohol one. The reaction proceeds continuously with time under the continuous mixing (64 or 84 rpm) and goes slower with a lower mixing speed (64 rpm). This is expected because a lower mixing speed should lead to a slower interfacial area

generation. Under the stepwise mixing (mixing mode b), the reaction proceeds in a stepwise manner: it pursues when there is mixing and stops when mixing stops. When there is no mixing all long (mixing mode c), there is no reaction over 90 min (see the horizontal line). These results suggest that the reaction in the heterogeneous macromolecular alcohol system is completely mixing-driven, and that once a new interfacial area is generated, the reaction between the complementary functional groups within the interface should occur very quickly. Moreover, there should exist an intermediate mixing speed between 0 and 64 rpm above which the overall rate of the heterogeneous reaction system exceeds that of the homogeneous one.

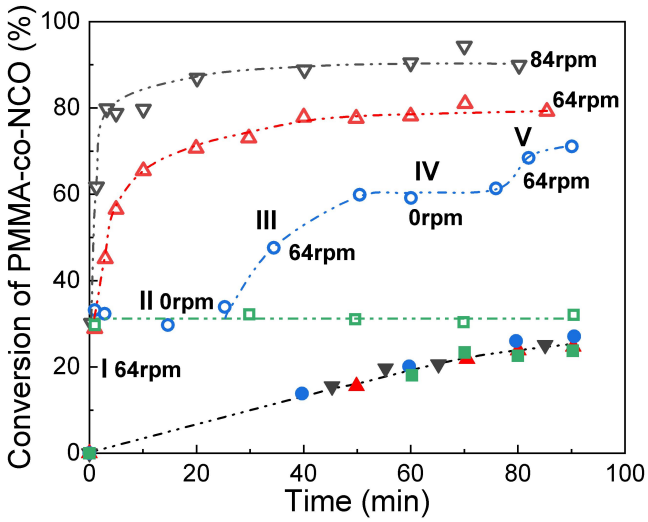

Figure 14. Comparison between a (PMMA+PMMA-r-NCO)/(PS+PS-CH_2CH_2-OH) heterogeneous reaction system (open symbols) and a (PMMA+PMMA-r-NCO)/Ph-$CH_2CH_2CH_2$-OH homogeneous reaction system (closed symbols) in terms of the conversion of the NCO group as a function of mixing time. Set temperature: 175°C; mixing modes: (a) continuous mixing at 64 or 84 rpm; (b) stepwise mixing alternating between 0 and 64rpm; (c) no mixing except for the very first minute during which the mixer turned at 64 rpm to ensure the melting and a certain degree of homogenization of the reaction systems. The dashed curves are drawn to guide the eye. Adapted from Feng and Hu [40].

To further analyze the the above finding, consider a second-order reaction between two complementary functional groups A and B in a volume V. Their molar numbers are n_A and n_B. If the reaction system is homogeneous, the reaction takes place over the entire volume V. If it is heterogeneous, the reaction only occurs in the interfacial volume V_i which is much smaller than V. The rates of reaction for both systems can be expressed by the following two equations:

For a homogeneous reaction system	$R_{ho} = k_{ho}[C_A]_{ho}[C_B]_{ho}V$	(16a)
For a heterogeneous reaction system	$R_{he} = k_i[C_A]_i[C_B]_i V_i$	(16b)

From the initial slopes of the curves under the continuous mixing in Figure 13, $R_{he}/R_{ho} \gg 1\ (\sim 10^2)$. Since $V_i/V \ll 1$ (suppose that it is $\sim 10^{-2}$), then $k_i[C_A]_i[C_B]_i/k_{ho}[C_A]_{ho}[C_B]_{ho} \gg 1\ (\sim 10^4)$. Unless $[C_A]_i[C_B]_i/[C_A]_{ho}[C_B]_{ho} \gg 1(\sim 10^4)$, one would have to conclude that $k_i/k_{ho} \gg 1$. Chain ends tend to enrich at the interfaces between immiscible polymers for entropic reasons, consequently their concentrations at the interfaces are higher than those in the bulk phases [44]. Nevertheless, the interfacial enrichment generally should rarely increase the concentrations of the functional groups by more than a factor of 2 [45, 46], even in an equilibrium state without flow/mixing. Thus, $k_i/k_{ho} \gg 1\ (\sim 10^2 - 10^3)$, meaning that the interfacial reaction constant is three orders of magnitude higher than the homogeneous reaction constant.

The above assumption that the interfacial reaction rate constant can be two or three orders of magnitude higher than the homogeneous reaction constant can be plausible. When two complementary functional groups are attached to two small molecules, they can easily collide with each other but can also easily walk way from each other. By contrast, when they are attached to polymer chains of different chemical nature and are confined inside an interface to within a capture radius R_c (see Figure 15a), they are then condemned to collide and react with each other because they cannot easily move away from each other due to the interfacial confinement. This may be called *interfacial confinement enhanced reactivity*. However, complementary functional groups which are confined inside an interface but are located over a distance greater than the capture radius as well as those which are located away from the interfaces may need a very long time to come to within the capture radius. The role of mixing is to bringing them to within the capture radius through advection and diffusion enhancement (Figure 15b). The interfacial confinement enhanced reactivity of functional groups together with mixing-driven interfacial area generation are the fundamental bases of the commercial success of reactive polymer blending [47].

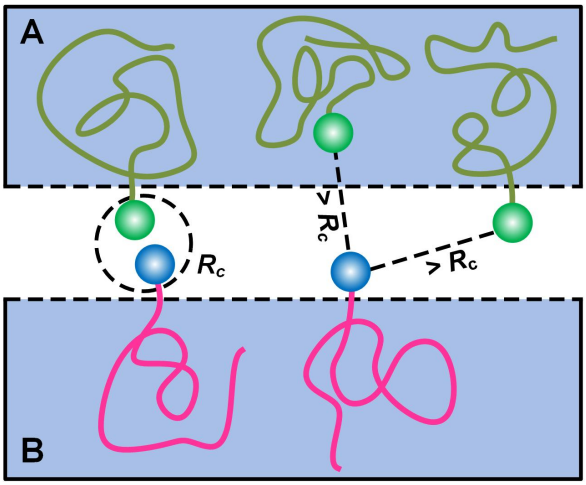

Figure 15. A schematic representation of two types of complementary functional groups within and away from an interface between two immiscible polymers A and B. One notices three scenarios: two complementary functional groups located inside the interface within a capture radius R_c; two complementary functional groups located inside the interface with a distance larger than the capture radius; complementary functional groups located away from the interface.

In short, both the theoretical developments and experimental observations described above provide understanding in support of the scientific and technical interests of flow-driven chemistry. However, the understanding is fragmented and scarce. Moreover, there is a mismatch between theories and experiments: the former address almost exclusively the effects of 1D flow on diffusion-controlled chemical reactions in homogeneous systems, whereas most experiments study the effects of mixing (3D flow) on chemical reactions in heterogeneous systems and a very few on the effects of 1D flow on chemical reactions in homogeneous systems. Most importantly, there are no well-controlled experiments which allow quantifying in an irrevocably the effects of a flow-driven change in molecular dynamics on the reaction kinetics and/or selectivity.

6. PERSPECTIVES

The essence of flow-driven chemistry is to modulate the dynamics (or the state of non-equilibrium) of molecules via a specific flow field in order to tune the reaction kinetics and/or selectivity. Based on the state of the art of the understanding related to flow-driven chemistry, the following research directions and methods are proposed in order to gain further understanding:

(a) It is absolutely crucial to conduct well-controlled experiments in order to irrevocably reveal and highlight the effects and interests of 1D flow on reaction kinetics and/or selectivity. A well-controlled experiment should meet at least three criteria: (i) A well-defined simple flow field. A co-axial cylindrical reactor could do the job. (ii) Chemical reactions should be irreversible. The reaction between an amine group and an isocyanate group can be a good candidate. (iii) Reaction systems are homogeneous under the reaction conditions.

(b) Irreversible coupling reactions between two rod-like *mono*-functional molecules could be the best candidates as they are expected to be most sensitive to a linear flow.

(c) Rod-like mono-functional molecules may then be extended to flexible *mono*-functional analogues which are expected to require a stronger flow to detect its effects on the reaction kinetics.

(d) Mono-functional molecules may subsequently be extended to rod-like and flexible *bi*-functional molecules which can be good candidates for studying the effects of 1D flow on the competition (selectivity) between irreversible intermolecular coupling (chain growth) and irreversible intramolecular coupling (cyclization).

(e) It is very important to characterize and model the conformations, dynamics, structural order and collision of molecules under flow [48-50], including interfaces for immiscible systems [45].

Among potential industrial impacts of flow-driven chemistry, one may mention:

(a) cases where cyclization reactions are undesirable. For example, polycondensation often involves cyclization [51]. The presence of cyclic molecules in polymers greatly jeopardizes its applications.

(b) Chemical reactions may be extended to physical reactions such as flocculation and crystalization processes [52, 53]. Their kinetics and pathways can also be strongly influenced by flow.

7. CONCLUSIONS

This paper has proposed flow-driven chemistry which aims at controlling the kinetics and/or selectivity of chemical reactions by modulating molecular dynamics, structural order and collisions via a specific flow field. In other words, flow-driven chemistry is to use a strong flow to perturb molecular conformations so that reactions occur in a non-equilibrium state in favor of faster rates and/or higher selectivity. As outlined in the literature [54], kinetics of chemical reactions in an equilibrium state are fairly understood. However, those in a non-equilibrium state are poorly understood. Indeed, flow-driven chemistry faces many scientific challenges. Among them are the dynamics, structural order and collisions of molecules under

flow [55-56]. Flow-driven chemistry also faces technical challenges. One of them is how to significantly change molecular conformations in a feasible and controllable manner, especially when molecules are small. The existing literature provides useful but very limited and fragmented information related to flow-driven chemistry. In addition to theoretical developments on molecular dynamics, structural order and collisions under flow, well-controlled experiments are crucial for revealing and highlighting the fundamentals of flow-driven chemistry. Its industrial potentials are also need to be demonstrated.

References:

1. J. M. Ottino. Mixing and chemical reactions: A Tutorial. Chem. Eng. Sci. 1994;49:4005-4027.
2. Mara Guidi, Peter H. Seeberger, Kerry Gilmore. How to approach flow chemistry. Chem. Soc. Rev. 2020; 49:8910-8932.
3. Yongjin Cui,Jing Song,Chencan Du,Jian Deng,Guangsheng Luo. Determination of the kinetics of chlorobenzene nitration using a homogeneously continuous microflow. AIChE J. 2022;68:e17564
4. D. Moore, S. T. Cui, H. D. Cochran, P. T. Cummings. Rheology of lubricant basestocks: A molecular dynamics study of C30 isomers, J. Chem. Phys.2000;113:8833-8840.
5. Thomas A. Hunt, B. D. Todd. Diffusion of linear polymer melts in shear and extensional flows. J. Chem. Phys. 2009;131:054904.
6. Carreau, P. J. Rheological equations from molecular network theories. Transactions of The Society of Rheology 1972; 16: 99–127.
7. Yasuda, K. Investigation of the analogies between viscometric and linear viscoelastic properties of polystyrene fluids. PhD thesis 1979, Massachusetts Institute of Technology.
8. S. Bair, W. O. Winer. A quantitative test of the Einstein-Debye relation using the shear dependence of viscosity for low molecular weight liquids. Tribol. Lett. 26(3), 223–228 (2007).
9. S. Bair and T. Yamaguchi, “The equation of state and the temperature, pressure, and shear dependence of viscosity for a highly viscous reference liquid, dipentaerythritol hexaisononanoate,” J. Tribol. 139(1), 011801 (2017).

10. Prince E. Rouse. A Theory of the Linear Viscoelastic Properties of Dilute Solutions of Coiling Polymers. J. Chem. Phys.1953; 21:1272-1280.

11. M. Doi, S.F. Edwards. The theory of polymer dynamics. Oxford University Press, New York.

12. De Gennes, P.G. Reptation of a Polymer Chain in the Presence of Fixed Obstacles. J. Chem. Phys. 1971; 55:572-579.

13. De Gennes, P.G. Entangled Polymers. Physics Today 1983; 36, 6, 33-39 (1983)

14. Liu, P.; Lu, J.; Yu, H.; Ren, N.; Lockwood, F.E.; Wang, Q.J., Lubricant shear thinning behavior correlated with variation of radius of gyration via molecular dynamics simulations, J. Chem. Phys. 2017; 147:084904.

15. J. T. Padding, W. J. Briels. Zero-shear stress relaxation and long time dynamics of a linear polyethylene melt: A test of Rouse theory. J. Chem. Phys. 2001；114：8685-8693.

16. Jagadeesh Anmala, Vivek Kapoor. Mixing and Bimolecular Reaction Kinetics in a Plane Poisseulle Flow. Flow Turbulence Combust (2012) 88:387–405

17. Nicholas B Engdahl, David A Benson, Diogo Bolster. Predicting the enhancement of mixing-driven reactions in nonuniform flows using measures of flow topology. Phys.Rev. E 2014; 90:051001(R).

18. A. Paster, T. Aquino, D. Bolster. Incomplete mixing and reactions in laminar shear flow. Phys.Rev.E 2015; 92:012922.

19. P. G. de Gennes, Kinetics of diffusion-controlled processes in dense polymer systems. I. Nonentangled regimes, J. Chem. Phys. 76, 3316-3321 (1982)

20. P. G. de Gennes, Kinetics of diffusion-controlled processes in dense polymer systems. II. Effects of Entanglements, J. Chem. Phys. 76, 3322-3326 (1982)

21. Glenn H. Fredrickson, Ludwik Leibler. Theory of Diffusion-Controlled Reactions in Polymers under Flow. Macromolecules 1996, 29, 2674-2685.

22. Alexander Kolb, Carlos M. Marquesa, Glenn H. Fredrickson. Flow effects in the polymer cyclization reaction. Macromol. Theory Simul. 1997; 6:169-180.

23. Sumeet Jain, Ameya Agge, and D. V. Khakhar. Flow enhanced diffusion-limited polymerization of rodlike molecules. J. Chem. Phys. 2001; 114:553-560.

24. Mary M. Caruso, Douglas A. Davis, Qilong Shen, Susan A. Odom, Nancy R. Sottos, Scott R. White, Jeffrey S. Moore. Mechanically-Induced Chemical Changes in Polymeric Materials. Chem. Rev. 2009, 109, 5755–5798.

25. Bell George I. Models for the specifific adhesion of cells to cells. Science 1978; 200:618–627

26. Changbong Hyeon, D Thirumalai. Measuring the energy landscape roughness and the transition state location of biomolecules using single molecule mechanical unfolding experiments.J. Phys.: Condens. Matter 2007; 19:113101.

27. Zhen Huang and Roman Boulatov. Chemomechanics with molecular force probes. Pure Appl. Chem. 2010; 82: 931–951.

28. G. Lebon, J. Casas-Vázquez, D. Jou, M. Criado-Sancho. Polymer solutions and chemical reactions under flow: A thermodynamic description. J. Chem. Phys. 1993; 98:7434-7439.

29. Ji Zhou, Wei Yu, Chixing Zhou. Rheokinetic study on homogeneous polymer reactions in melt state under strong flow field. Polymer 2009; 50:4397–4405.

30. Tuuli A. Hakala, Emma V. Yates, Pavan K. Challa, Zenon Toprakcioglu, Karthik Nadendla, Dijana Matak-Vinkovic, Christopher M. Dobson, Rodrigo Martínez, Francisco Corzana, Tuomas P. J. Knowles, Goncalo J. L. Bernardes. Accelerating Reaction Rates of Biomolecules by Using Shear Stress in Artifificial Capillary Systems. J. Am. Chem. Soc. 2021; 143:16401−16410.

31. U. S. Agarwal, D. V. Khakhar. Enhancement of polymerization rates for rigid rod-like molecules by shearing. Nature 1992; 360: 53-55.

32. Zhangcheng Gao, Jianqing Wang, Lianfang Feng, Xueping Gu, Jintang Duan, Cailiang Zhang. Flow-accelerated polycondensation reaction to prepare rigid rodlike poly (p-phenylene-cis-benzobisoxazole). Chemical Engineering and Processing - Process Intensification 2022: 176:108972.

33. Hyun K. Jeon, Christopher W. Macosko, Bongjin Moon, Thomas R. Hoye, Zhihui Yin. Coupling Reactions of End- vs Mid-Functional Polymers. Macromolecules 2004; 37:2563-2571.

34. Christopher W. Macosko, Hyun K. Jeona, Thomas R. Hoye. Reactions at polymer–polymer interfaces for blend compatibilization. Prog. Polym. Sci. 2005; 30: 939–947.

35. Orr CA, Cernohous JJ, Guegan P, Hirao A, Jeon HK, Macosko CW. Homogeneous reactive coupling of terminally functional polymers. Polymer 2001; 42:8171.

36. Jianbin Zhang, Shengxiang Ji, Jie Song, Timothy P. Lodge, and Christopher W. Macosko. Flow Accelerates Interfacial Coupling Reaction.Macromolecules 2010; 43:7617–7624.

37. Jie Song, Adam M. Baker, and Christopher W. Macosko. Reactive Coupling between Immiscible Polymer Chains: Acceleration by Compressive Flow. AIChE Journal 2013; 59:3391-3402.

38. Zheng, X.; Rafailovich, M. H.; Sokolov, J.; Strzhemechny, Y.; Schwarz, S. A.; B., S.; Rubinstein, M. Long-Range Effects on Polymer Diffusion Induced by a Bounding Interface. Phys. Rev. Lett. 1997; 79:241-244.

39. Odian, G. Principles of Polymerization. Wiley-Interscience, New York (1981).

40. Lian-Fang Feng, Guo-Hua Hu. Reaction Kinetics of Multiphase Polymer Systems under Flow. AIChE journal 2004; 50:2604-2612

41. Guo-Hua Hu, Morand Lambla. Chemical reactions between immiscible polymers in the melt: Transesterification of poly (ethylene-co-methyl acrylate) with mono-hydroxylated polystyrenes. J. Polym. Sci. Part A: Polym. Chem. 1995; 33:97-107.

42. Hu, G. H., and Kadri, I. Modeling Reactive Blending: An Experimental Approach. J. Polym. Sci. Polym. Phys. Ed.1998; 36:2153-2163.

43. Hu, G. H., and Kadri, I. Preparation of Macromolecular Tracers and Their Use for Studying the Residence Time Distribution of Polymeric Systems. Polym. Eng. Sci.1999; 39:299-311.

44. F. Schimid, M. Muller. Quantitative comparison of self-consistent-field theories for polymers near interfaces with Monte-Carlo simulations. Macromolecules 1995; 28: 8639-8645.

45. Sandra Barsky, Mark O. Robbins. Molecular dynamics study of slip at the interface between immiscible polymers. Phys. Rev.E 2001; 63:021801.

46. Narayan P. Adhikari, Ekkehard Straube. Interfacial Properties of Asymmetric Polymer Mixtures. Macromol. Theory Simul. 2003, 12, 499–507.

47. Warren Baker, Chris Scott, Guo-Hua Hu. Reactive Polymer Blending. Hanser, 2001.

48. Philip LeDuc, Charbel Haber, Gang Bao, Denis Wirtz. Dynamics of individual flexible polymers in a shear flow. Nature 1999; 399:564-566.

49. Omar Castrejon-Gonzalez, Jorge Castillo-Tejas, Octavio Manero, Juan F. J. Alvarado. Structure factor and rheology of chain molecules from molecular dynamics. J. Chem. Phys. 2013; 138: 184901

50. Andrew J. Orr-Ewinga. Perspective: Bimolecular chemical reaction dynamics in liquids. J. Chem. Phys.2014; 140:090901.

51. Hans Kricheldorf. Polycondensation - History and new results. Springer Berlin, Heidelberg, 2004.

52. Zhenbei Wang, Jun Nan, Xiaoyu Ji, Yueming Yang. Effect of the micro-flocculation stage on the flocculation/sedimentation process: The role of shear rate. Science of The Total Environment 2018; 633: 1183-1191.

53. Carol Forsyth, Paul A. Mulheran, Claire Forsyth, Mark D. Haw, Iain S. Burns, and Jan Sefcik. Inflfluence of Controlled Fluid Shear on Nucleation Rates in Glycine. Cryst. Growth Des. 2015; 15:94−102.

54. Eli Pollak, Peter Talkner. Reaction rate theory: What it was, where is it today, and where is it going? CHAOS 2005; 15:026116.

55. Takeshi Sato, Youngdon Kwon, Yumi Matsumiya. A constitutive equation for Rouse model modified for variations of spring stiffness, bead friction, and Brownian force intensity under flow. Phys. Fluids 2021; 33:063106.

56. Scott T. Milner. Unifified entanglement scaling for flexible, semiflflexible, and stiffff polymer melts and solutions. Macromolecules 2020; 53:1314−1325.